

DAVID BLOOM

Larry Mayer  
Department of Geology  
Miami University  
Oxford, Ohio 45056

13

SUBSIDENCE ANALYSIS  
OF THE LOS ANGELES  
BASIN

309

## ABSTRACT

Subsidence analysis of the central block of the Los Angeles basin, using backstripping techniques, shows two distinct periods of tectonic subsidence. The first occurred about 28 my B.P. and was synchronous with increased sedimentation that kept the basin filled. The second period of tectonic subsidence occurred about 12 my B.P. and was synchronous with widespread andesitic and basaltic volcanism. Sedimentation, however, lagged behind, resulting in a deep, water-filled basin. Water depths may have been in excess of 2 km during the Pliocene. After 5 my B.P., a pulse of sedimentation filled the basin, causing some further subsidence of the basin floor, but this was due only to sediment-induced loading of the lithosphere. The rapid sedimentation in the central block during the Late Pliocene may be the signal of the modern big bend in the San Andreas fault and its associated uplifts. Assuming Airy isostatic mechanisms, lithospheric thinning on the order of 50-75% under the central deep accounts for the observed tectonic subsidence.

## INTRODUCTION

The Los Angeles basin is strategically situated, in the sense that it is located near the point of initial encounter of the East Pacific Rise and the trench at the western margin of the North American plate, and was, therefore, at the locus of intense wrench tectonism. Transform faulting and associated wrenching have resulted in a structurally complex basin with remarkably high subsidence rates and a prolific petroleum production history. This paper summarizes salient aspects of the history of the Los Angeles basin and attempts to provide some new insights by means of subsidence analysis.

The purpose of subsidence analysis is to relate subsidence, sedimentation, and thermal characteristics to the timing and magnitude of lithospheric thinning. Subsidence analysis permits the partitioning of total subsidence into that part due to sediment loading, and a residual subsidence, which is often referred to as tectonic subsidence. The delineation of tectonic subsidence allows comparisons between theoretical subsidence histories based on rifting models and calculated tectonic subsidence for a given basin. Use of the method here is aimed at unravelling a complicated basin history and at determining whether basins formed in wrench settings have a particular subsidence pattern. Many of the fine details have been omitted unless directly relevant.

## SETTING

The Los Angeles basin is situated at the northern end of the Peninsular Ranges geomorphic province and in a general way, is bounded on the north by the Transverse Ranges geomorphic province (Fig. 13-1). The history of the basin was profoundly influenced by evolution of the San Andreas fault system. The development of the San Andrea fault has been studied by Atwater (1970), Atwater and

300



Fig. 13-1. Location diagram showing place names and major faults referred to in this report.

Molnar (1973) and many others, and reviewed by Coney (1979). Prior to about 30 my BP, the Farallon plate, consisting of dominantly young oceanic lithosphere, was being subducted along a trench along the western margin of North America at a shallow but increasingly high angle (Coney and Reynolds, 1977; Dickinson and Snyder, 1978; Keith, 1978).

About 29 my B.P., part of the East Pacific Rise encountered the trench. The resolution of relative plate motions resulted in right-lateral transform motion along an early San Andreas fault, which was born at the point of interaction, and subsequently extended northward with the transform-transform-trench triple junction (Atwater, 1970). The early San Andreas fault (where "early" denotes the period between 29 and 12 my B.P. and is distinct from the notion of the proto-San Andreas, which generally refers to its Cretaceous and Paleocene history) may have been a very wide zone of strike-slip and extensional faulting (Atwater, 1970).

The extent of the early San Andreas system and its evolution into the present fault pose many problems because of the resultant complicated structural patterns. Palinspastic reconstructions are difficult and various "stress" regimes have been suggested. Many models, for example, have been proposed to explain east-west crustal extension in Middle Miocene time (e.g., Atwater, 1970; Campbell and Yerkes, 1971, 1976; Yeats, 1973, 1976b; Crowell, 1974a) in southern California,

301

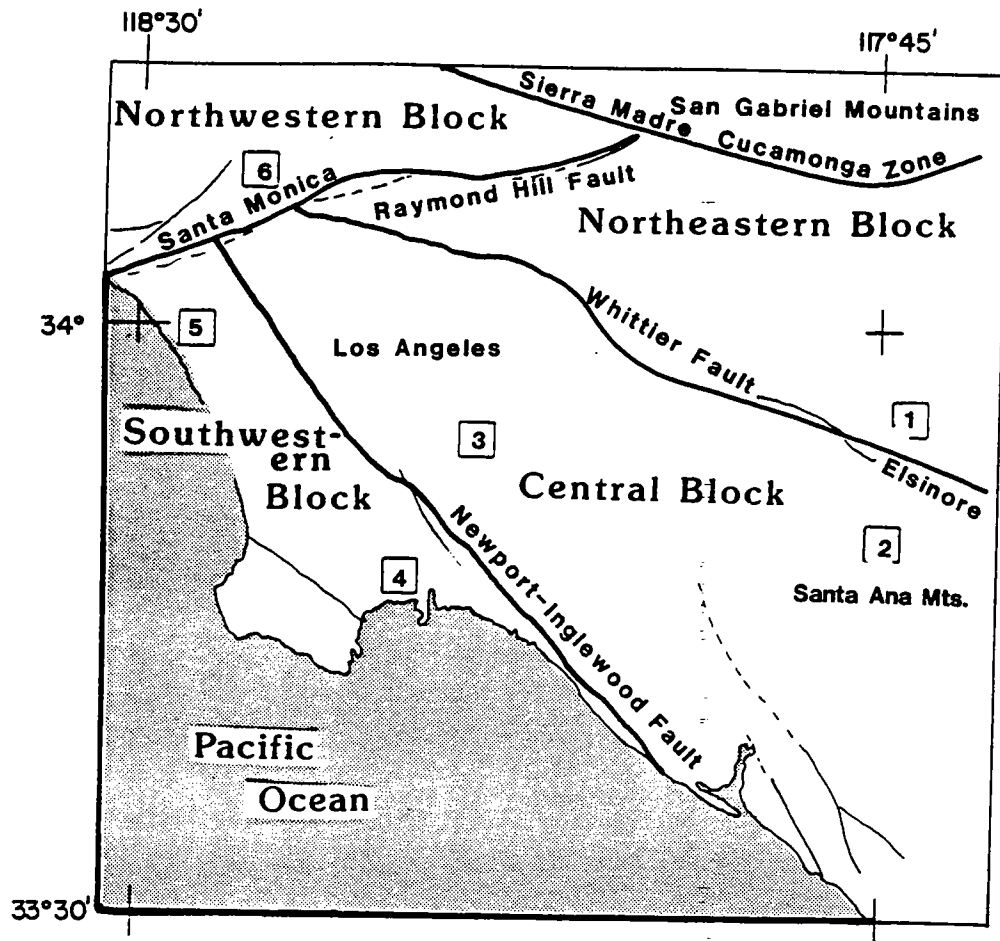


Fig. 13-2. Subdivisions of the Los Angeles basin. Boxed numbers refer to the locations of well data. After Yerkes, et al. (1965).

but the problem of a comprehensive palinspastic reconstruction is largely unresolved. The problem is further complicated by apparent discrepancies between the movement history of the present San Andreas, and the much greater slip predicted from relative plate motions. In addition, the San Andreas fault north and south of the Transverse Ranges exhibits different displacement histories (Dickinson *et al.*, 1972; Graham, 1978; Nardin and Henyey, 1978). Because slip histories of the regional and local faults are of vital concern to the evolution of the Los Angeles basin, a summary is given in Appendix 1.

The Los Angeles basin is subdivided into four distinct fault-bounded blocks (Yerkes *et al.*, 1965). The Newport-Inglewood fault separates the central from the southwestern block, whereas the Whittier fault and Santa Monica-Cucamonga system (see Appendix 1 for slip history) define the boundaries among the northeastern, northwestern and bounding blocks (Fig. 13-2). These faults, presumably, have allowed each block to have a different subsidence history and also a different basement configuration (Fig. 13-3).

Og: spelling?

(208)

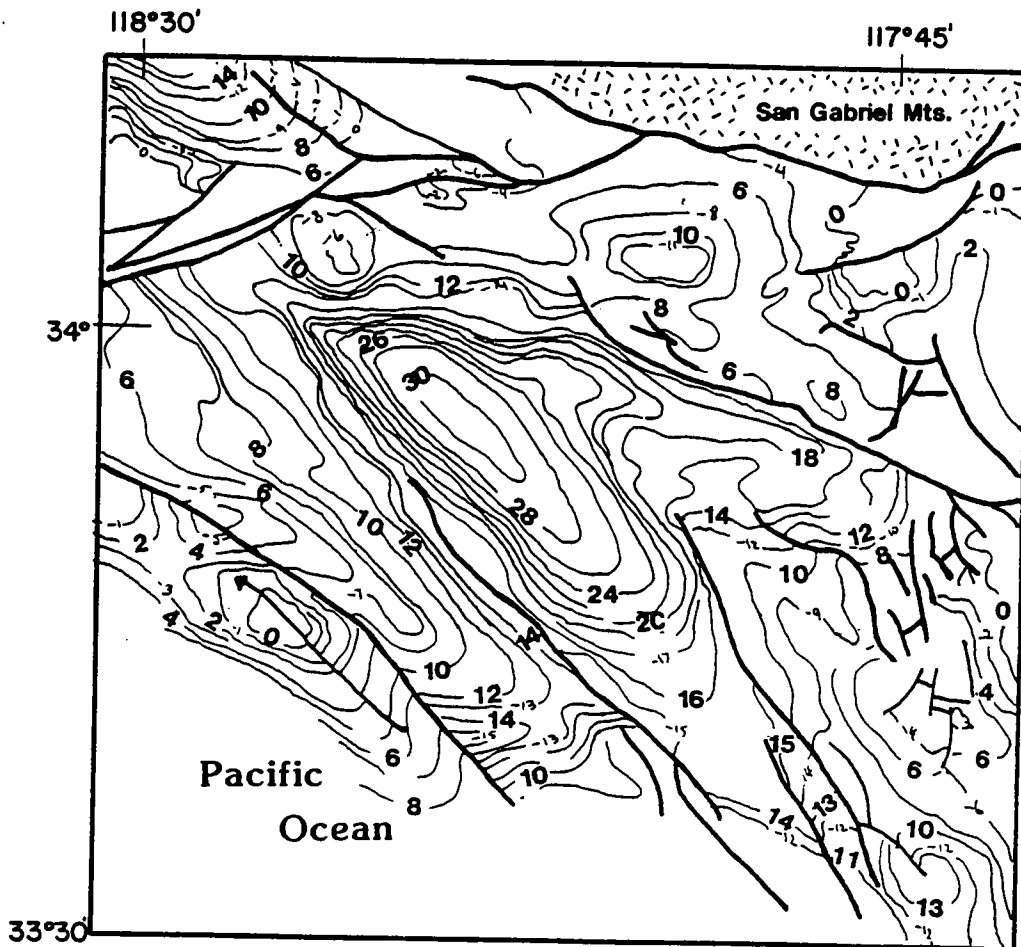


Fig. 13-3. Depth to basement map of the Los Angeles basin. Contours are in thousands of feet. From Yerkes, et al. (1965).

### SUBSIDENCE ANALYSIS

The purpose of subsidence analysis is to reconstruct the history of subsidence and sedimentation in a basin using the sedimentary record. The procedure is complicated by compaction of sediments, changes in paleobathymetry, and loading-induced subsidence. Figure 13-4 illustrates the simplest case of subsidence analysis, where only sedimentation and tectonic subsidence are considered. The time slice at  $t_4$  represents a stratigraphic section as it exists today, perhaps obtained from well data. The idea is to predict what the elevation of the basin floor would be at times  $t_0$ - $t_3$  in the past. In this simplified case, all we need to know is the thicknesses of units 1-4. To find the amount of subsidence at time  $t_3$ , we simply remove unit 4 and allow the basin floor to move up by an amount equal to the thickness of unit 4. This case is overly simple because sedimentation is equal to the amount of



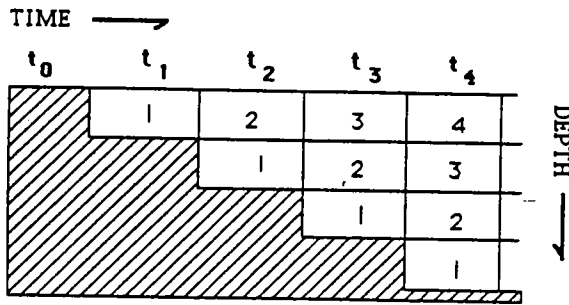


Fig. 13-4. Time slices in the subsidence history of a hypothetical basin.  $t_0$  is the initial condition. Patterned area is basement.

tectonic subsidence, but it illustrates the logic of using stratigraphic data to determine subsidence history.

Figure 13-5 illustrates a more realistic situation where water depth, sedimentation rate, and compaction all operate to make the simple procedure, used above, unworkable. For example, if we removed the uppermost sediments at time  $t_4$ , then we would predict a basin history much different than the actual one shown at time  $t_3$ . Clearly, information on paleobathymetry is important. Also, we need a way to "decompact" sediments back to their depositional thicknesses rather than use compacted thicknesses. Finally, we need a way to distinguish subsidence that is tectonic in origin from subsidence caused by sediment loading. Techniques to accomplish this have been referred to as "geohistory analysis" (Van Hinte, 1978) or "backstripping" (Steckler and Watts, 1978).

In a setting where a basin can be considered to respond to loading by Airy mechanisms, it is rather straightforward to account for loading subsidence. This concept is shown in Fig. 13-6. The scale represents the mechanism of Airy isostasy, and when the amount of subsidence due to loading alone is removed, there is a residual subsidence. This residual is the tectonic subsidence that formed the initial basin. The equation that is used to calculate tectonic subsidence is derived from balancing Airy columns and is shown in Fig. 13-7.

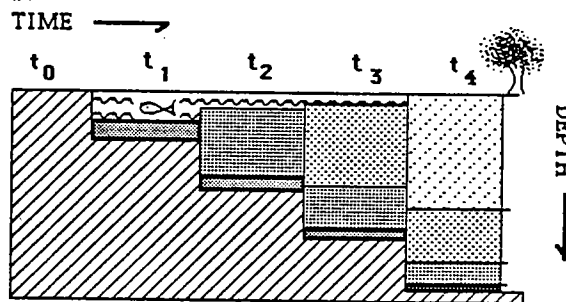
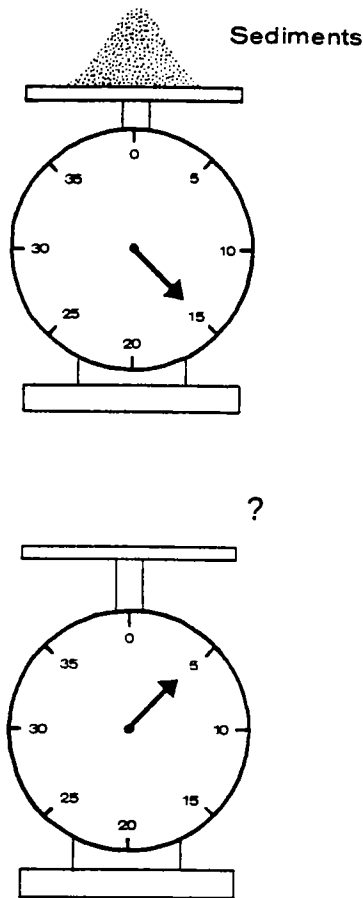


Fig. 13-5. Time slices in the subsidence history of a hypothetical basin. Here, water depth, sedimentation rates, and compaction all vary with time.

305

## BACKSTRIPPING

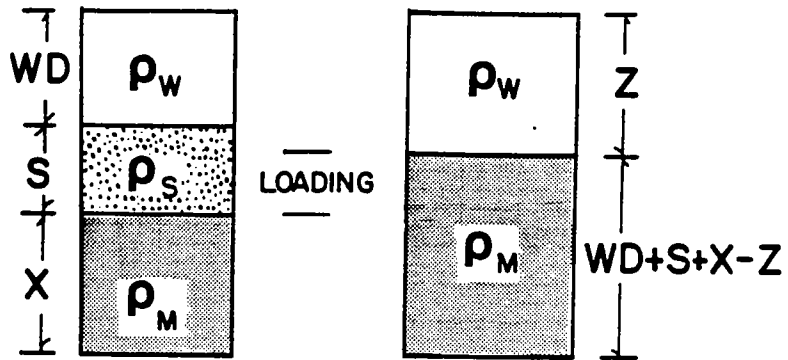
Fig. 13-6. Conceptual rendering of backstripping technique. The mechanism for the scale is isostasy. When the weight of sediment is removed, there is a residual subsidence.



Backstripping techniques can account for porosity reductions due to cementation alone or cementation and compaction (Mayer, 1982; Bond and Kominz, 1984). Compaction corrections are applied by computing the net thickness of a horizon (i.e., zero porosity), and using this net thickness with the porosity-depth curve from the well to adjust for depth-dependent density changes (Horowitz, 1976). As each progressively younger stratigraphic unit is removed from the stack of sediments, a new sediment density is calculated based on decompaction corrections derived from porosity-depth functions for the different rock types. These densities, in turn, are used in the calculation of tectonic subsidence.

Recall that the three data components needed for subsidence analysis are age, thickness, and paleobathymetry of each sedimentary unit. The subsidence history of the central block is described because it has the thickest and presumably the best-preserved record of sedimentation.

306



### Backstripping Sediment Loading

Balance Columns:

$$\rho_w WD + \rho_s S + \rho_M X = \rho_w Z + \rho_M WD + \rho_M S + \rho_M X - \rho_M Z$$

$$Z = WD + S \left( \frac{\rho_M - \rho_s}{\rho_M - \rho_w} \right)$$

Fig. 13-7. Derivation of the backstripping equations. Z is the depth to the basin floor after sediment loading is removed. WD is water depth. S is the thickness of the sedimentary load.

## TECTONOSTRATIGRAPHY

The time scale used in this report is in general accord with the revisions presented by Turner (1970), Boellstorff and Steineck (1975) and Howell (1976). The Pliocene-Miocene boundary is placed at 5 my B.P. Stratigraphic data for the basin (from Yerkes *et al.*, 1965) are summarized on time-thickness bar diagrams (Mayer and Dickinson, 1984), which simultaneously display lithostratigraphic thickness and chronostratigraphic range (Figs. 13-8 to 13-13). Unconformities are seen as gaps between bars, whereas rapid sediment accumulation is represented by long narrow bars. This format accentuates tectonically related groups of sedimentary (tectonostratigraphic) units.

### Basement

In the northeastern block, basement consists of granodiorites of the southern California batholith, or in some places, metasedimentary and metavolcanic rocks. In the central block, rocks of the Bedford Canyon Formation are found. These

3076



# NORTHEASTERN BLOCK

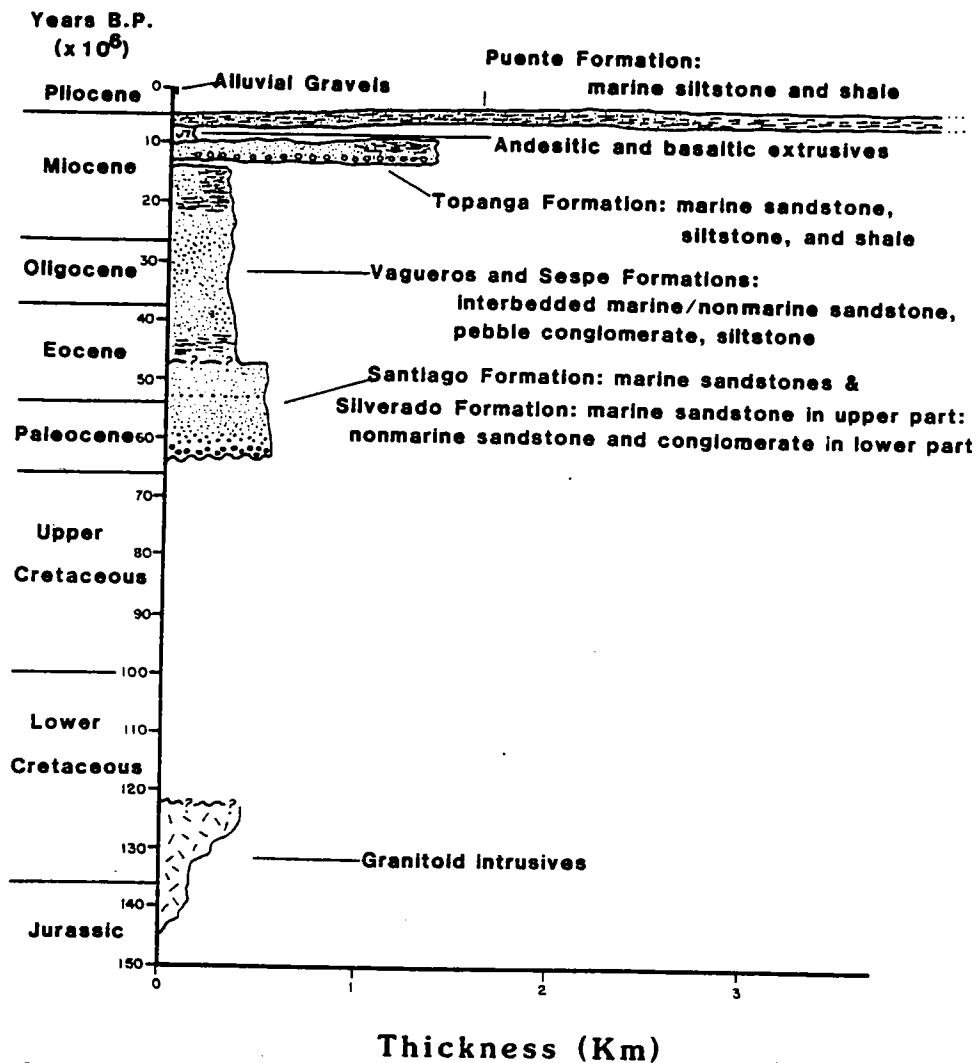


Fig. 13-8. Time-thickness bar diagram for well location 1. Data from Yerkes, *et al.* (1965).

are slightly metamorphosed, dark, well bedded sandstone and siltstone with well developed slaty cleavage, and intense folding and jointing (Yerkes *et al.*, 1965). The Bedford Canyon Formation is believed to be Jurassic (Imlay, 1963). Unconformably overlying the Bedford Canyon Formation are the Santiago Peak Volcanics. These are chiefly andesitic breccias, flows, agglomerates, and tuffs, all intensely altered (Yerkes *et al.*, 1965). The Santiago Peak Volcanics are intruded by the granodiorites of the southern California batholith of Cretaceous age (120 my based on lead-alpha methods; Larsen *et al.*, 1958).

308

# CENTRAL BLOCK

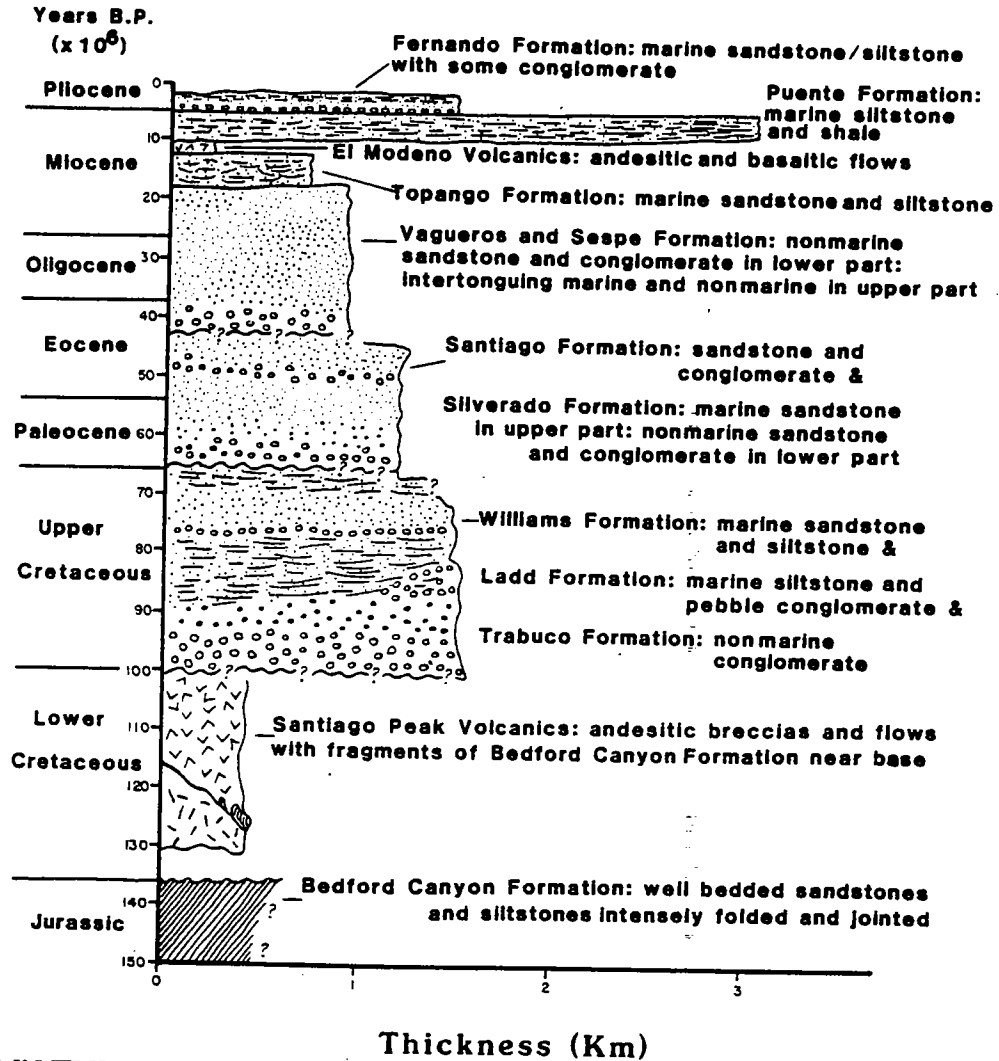


Fig. 13-9. Time-thickness bar diagram for well location 2. Data from Yerkes *et al.* (1965).

The northwestern block is underlain by the Santa Monica Slate of Late Jurassic age (Imlay, 1963). The Santa Monica slate is intruded by 122-my-old quartz diorites (Larsen *et al.*, 1958). The southwestern block is floored with Catalina Schist, which includes glaucophane-bearing schist containing epidote or zoisite and metavolcanics. The Catalina Schist is correlated with the Franciscan Complex of northern California (Woodford, 1924).

Yerkes *et al.*, (1965) refer to the basement of the southwestern block as

308

# CENTRAL BLOCK

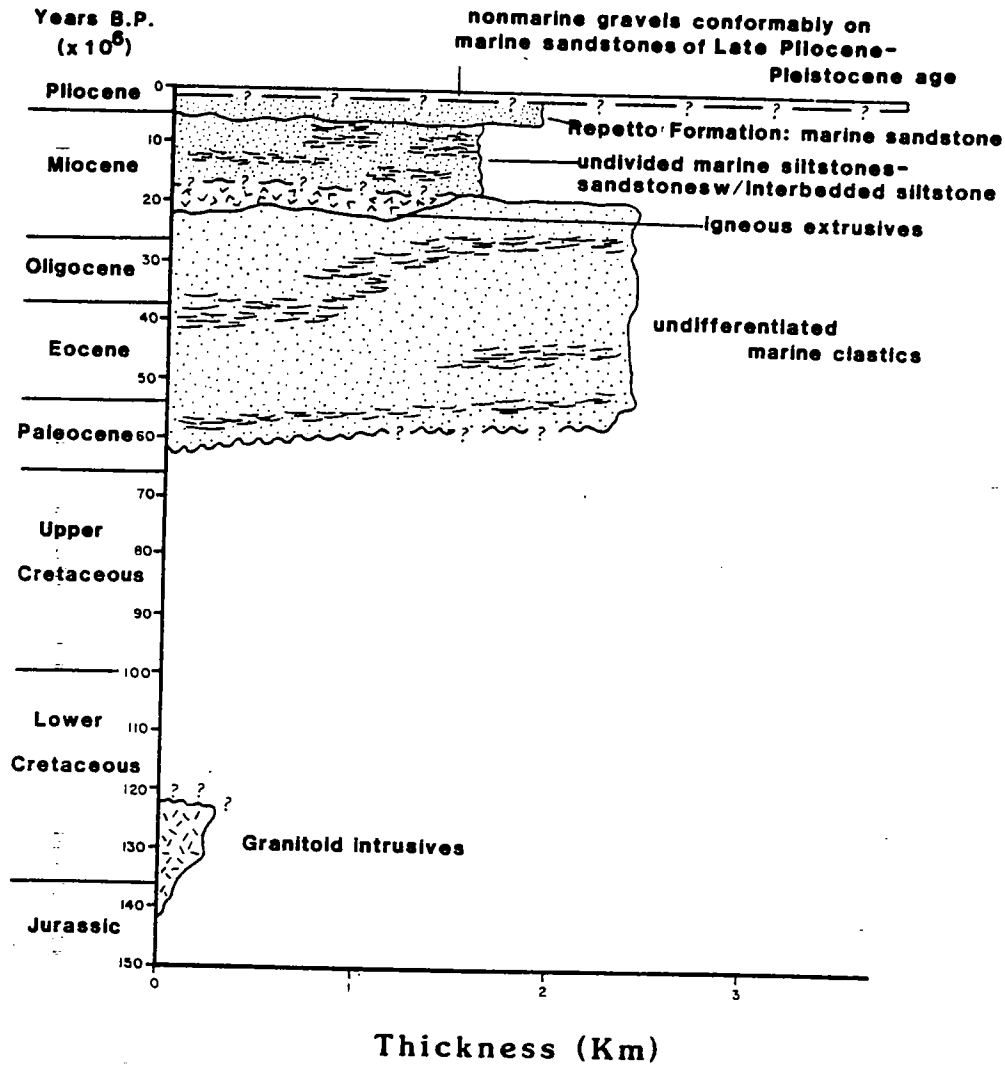


Fig. 13-10. Time-thickness bar diagram for well location 3. Data from Yerkes, et al. (1965).

“Western Basement”; it is tectonically distinct from the basement of the rest of the basin referred to as “Eastern Basement.”

## Units

The preserved stratigraphy in the Los Angeles basin permits the definition of three tectonostratigraphic units separated by three major unconformities. The definition

309

# SOUTHWESTERN BLOCK

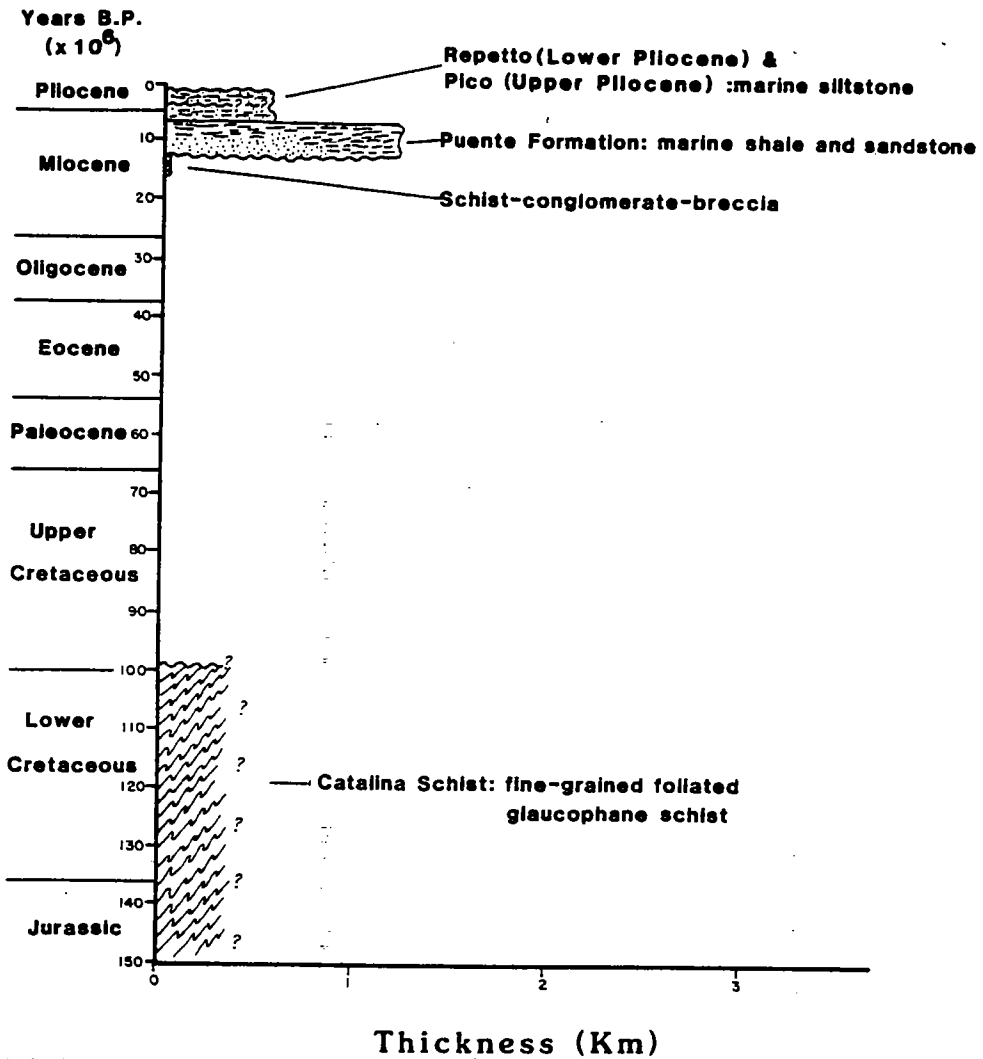


Fig. 13-11. Time-thickness bar diagram for well location 4. Data from Yerkes, et al. (1965).

of these packages is based largely on the interpretation of Figs. 13-8 to 13-13. The oldest unconformity is the Los Angeles erosion surface (Woodford and Gander, 1977) exposed in the Santa Ana Mountains. It occurs between the Santiago Peak Volcanics and the Turonian(?) Trabuco Formation. Post-mid-Cretaceous erosion has resulted in lengthening the time represented by this unconformity in other locations within the basin.

The oldest tectonostratigraphic unit sits on the Los Angeles erosion surface

# SOUTHWESTERN BLOCK

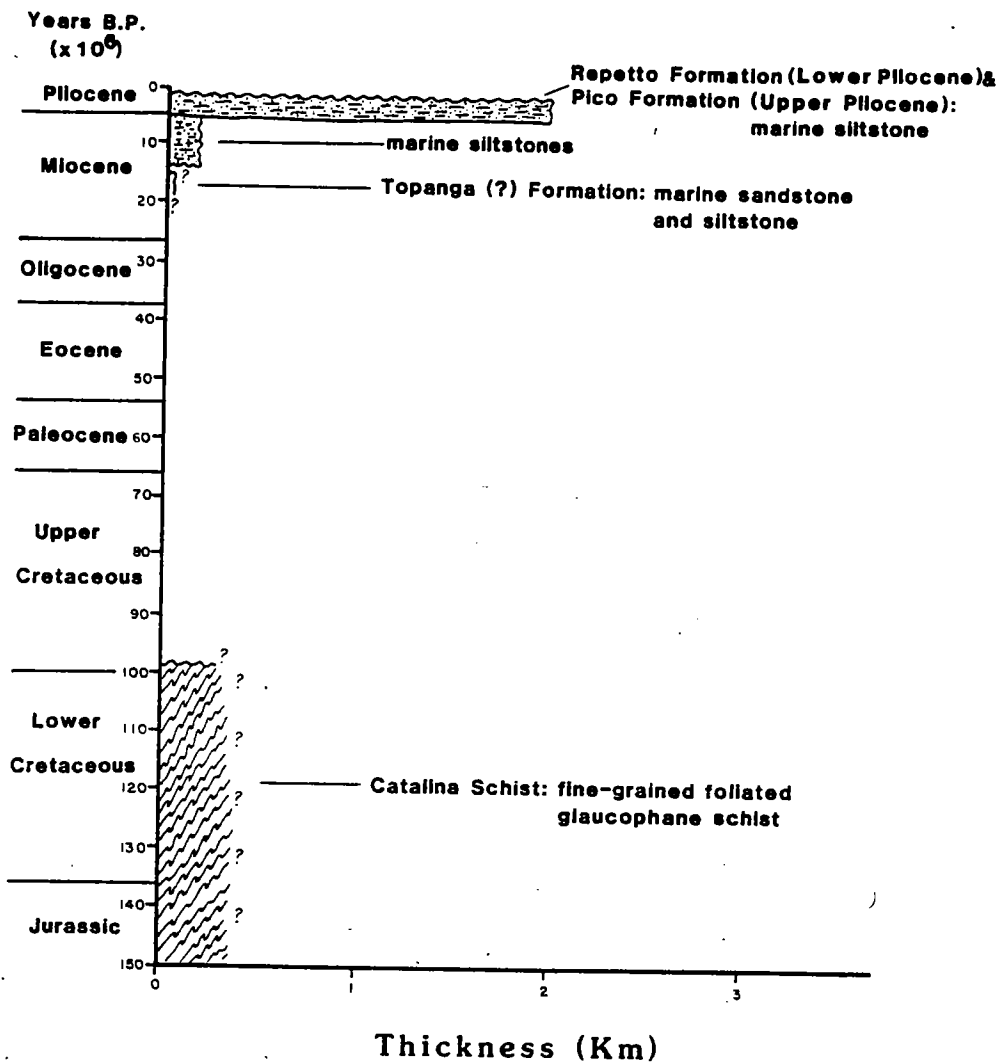


Fig. 13-12. Time-thickness bar diagram for well location 5. Data from Yerkes, et al. (1965).

and consists of nonmarine conglomerate of the Trabuco Formation (Figs. 13-9 and 13-13), and the shallow-marine sandstone, siltstone, and pebble conglomerate of the Ladd, Chico, and Williams formations. The boundary of this tectonostratigraphic unit is defined by the next important unconformity, which occurs at the Cretaceous-Paleocene boundary, although the exact duration of the time represented is unknown. A sequence of nonmarine arkosic sandstone of the Martinez Formation (Fig. 13-9), and marine and non-marine sandstone of the

311

# NORTHWESTERN BLOCK

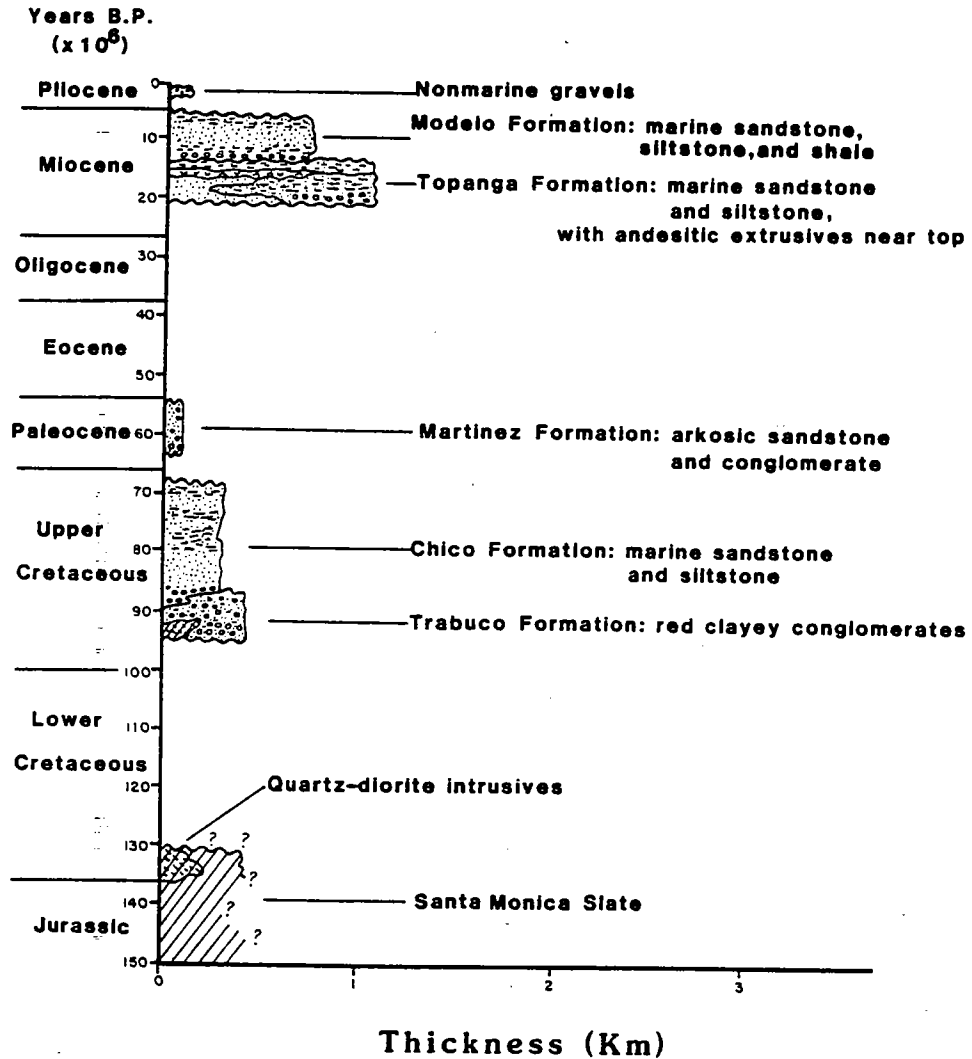


Fig. 13-13. Time-thickness bar diagram for well location 6. Data from Yerkes, et al. (1965).

Silverado, Santiago, Vaqueros, and Sespe formations form the next tectonostratigraphic unit.

The next younger unconformity is considered to be at the base of the Topanga Formation (Middle Miocene), except in the central block, where it is placed at the base of the Vaqueros Formation. The disparity in timing of this tectonostratigraphic unit among different blocks attests to the complicated

312

kinematics relating structural development to basin evolution. At location 3 (Fig. 13-10), igneous extrusives are reported: in the Santa Ana Mountains, mafic volcanics reach thicknesses up to 390 m (Woodford and Gander, 1977), and together with the Topanga, they define the next tectonostratigraphic unit. Widespread extrusion of andesitic and basaltic volcanics marks the beginning of the youngest, and perhaps, most significant tectonostratigraphic unit (Figs. 13-8, 13-9, and 13-13). Following this volcanism, a period of rapid sedimentation occurred, marked by a distinct spike on the time-thickness bar diagrams (Figs. 13-8 to 13-11). The "pairing" of volcanics with subsequent rapid subsidence may be a signal or "fingerprint" of extensional tectonics in a pull-apart basin. This youngest tectonic unit is particularly important because it contains the main oil-bearing strata.

### Paleobathymetry

Pre-Miocene water depths are inferred to have been shallow, based on the alternating sequences of nonmarine and marine sandstone, conglomerate and siltstone. Middle Miocene water depths in the Palos Verdes Hill area ranged from about 180 to 910 m (Woodring *et al.*, 1946), but the shallower-water forms may have been transported to deeper waters. Water depths for the Late Miocene may have reached 900 m, based on the presence of deep-water turbidites (Sullwold, 1960), or to 1300 m, based on foraminiferal and radiolarian assemblages (Ingle, 1980). However, Miocene foraminifera in the Santa Ana Mountains indicate 500 m of water depth in the early Middle Miocene, increasing rapidly to more than 1000 m (Natland and Rothwell, 1954) or perhaps even 2000 m (Ingle, 1980) by the end of the Late Miocene. A submarine sill is indicated for the south margin of the Puente Hills, and this is consistent with the Pliocene paleogeographic construction of Conrey (1967).

During the Early Pliocene, the submarine sill on the southwestern block may have reached depths of 1800 m; based on modern analogs, Conrey (1967) reasoned that the basin floor in the central block may have reached water depths of 2400 m. This latter figure is also consistent with Ingle's (1980) interpretation based on foraminifera. By the end of the Early Pliocene, the sill was about 1200 m deep (Conrey, 1967). The existence of a submarine sill on the northeastern and northern margins of the basin is supported by shallow water depths (180 m), reported by Vedder (1960) and the lithofacies studies of Conrey (1967).

---

### SUBSIDENCE HISTORY

The subsidence history of the central block of the Los Angeles basin is summarized in Fig. 13-14, which incorporates the information presented above, in addition to stratigraphic thicknesses from well data in the San Joaquin Hills (from Yerkes *et al.*, 1965). The data are plotted as a composite section that represents the deeper part of the central block. Figure 13-14 is patterned after the geohistory diagrams of Van Hinte (1978) and tectonic subsidence curves of Steckler and Watts (1978).

The bottom curve is the subsidence path of basement. The next higher curve is the tectonic subsidence curve, which is that portion of the basin's subsidence that cannot be explained by sediment loading and is derived by backstripping. Water loading is not shown, but lies in the area between the tectonic curve and the paleobathymetric curve, and represents the "complete" tectonic subsidence curve. The uppermost curve describes the paleobathymetry of the basin with time.

Prior to about 28 my B.P., the approximate time of deposition of the lower boundary of the Vaqueros, subsidence of the basin floor was slow, with little net tectonic subsidence. After 28 my B.P., the basin floor began to subside more rapidly, but sedimentation kept pace, and therefore, a deep-water basin did not develop. Sedimentation increased its rate slightly during the time of Topanga deposition in the interval from about 21 to 12 my B.P., but the rate of basin-floor subsidence increased by a larger amount, so that a deeper water-filled basin developed. Between 21 and 10 my B.P., the basin floor subsided at a very high rate. Relatively low sedimentation rates during deposition of the Monterey and Capistrano Formations (ca. 12-3 my B.P.), combined with a high subsidence rate, resulted in a very deep water-filled basin.

The basin continued to deepen until sometime during the Early Pliocene, perhaps 3 my B.P. The subsidence history from the Early Pliocene to the Pleistocene was characterized by continued subsidence of the basin floor, but also by a rapid pulse of sedimentation that filled the basin at a rate of about 1.5 km/my. The continued subsidence of the basin floor was entirely due to sediment loading,

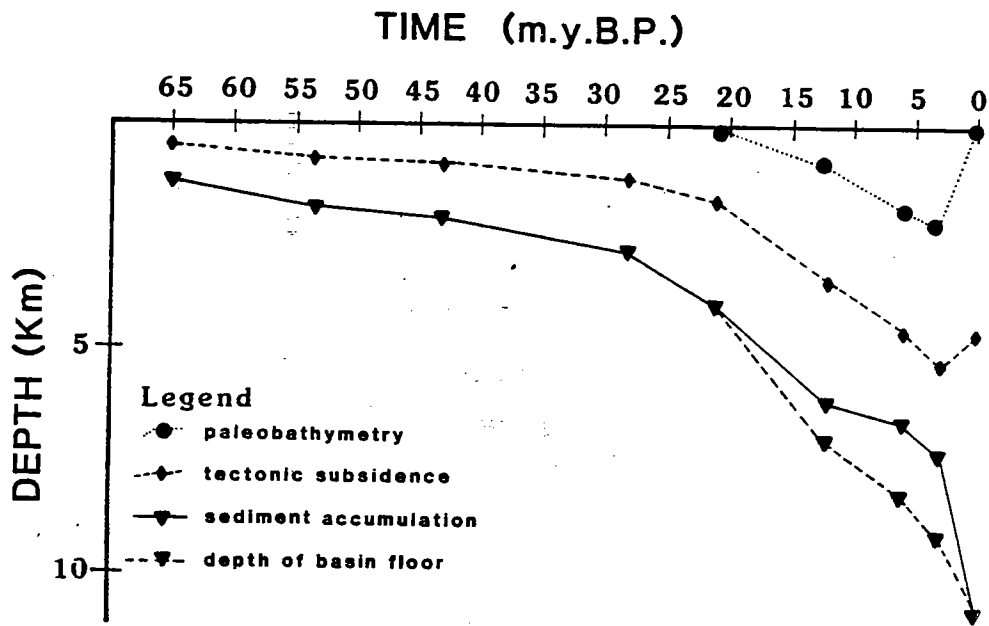


Fig. 13-14. Geohistory diagram illustrating the subsidence history of the Los Angeles basin central block.

314



unlike the San Joaquin Hills area, where uplift began about 3 my B.P. (Ingle, 1980). The trend of the complete tectonic-subsidence curve after 3 my B.P. in the deep part of the central block indicates that all tectonic subsidence had ceased.

The general pattern of subsidence (as shown on Fig. 13-14) and sedimentation (as shown on the time-thickness diagrams) seems to indicate two tectonic events, one at about 28 my B.P. and the second at about 12 my B.P. The older event is marked by an increase in the rate of tectonic subsidence. The younger event, though not seen as a distinct event on the subsidence curve, coincides with the start of deposition of the youngest tectonostratigraphic unit described above and corresponded with the peak of volcanism in the basin. Changes in rates of sedimentation and subsidence were not synchronous, and one may infer that the tectonic processes which affected these rates were somewhat independent. Basin subsidence has been related to pullapart structures, crustal attenuation (Crowell, 1974a), and thermal subsidence (Turcotte and McAdoo, 1979). The pulse of sedimentation during the Pliocene may be related to forces tending to form uplifts, such as the Transverse Ranges.

Two facts suggest that the pulse of sedimentation is related to the position of the modern big bend in the San Andreas system and related uplifts. First, rapid sedimentation requires uplifts of sufficient size and rate to provide enough sediments to fill the basin. These uplifts are presumably associated with compression across the big bend. It has been suggested that stress induced by the big bend was accommodated by the Malibu-Coast fault (Jahns, 1973). Second, tectonic subsidence either ceased or was reversed (i.e., uplift) at the time of most rapid sedimentation. This second fact appears to be consistent with the opening of the Gulf of California and the general northern movement of the Peninsular Ranges relative to the North American plate.

The size of the source area needed to fill the basin is dependent on erosion rates. Present erosion rates in the San Gabriel Mountains, part of the sediment source for the basin since Miocene time (Yerkes *et al.*, 1965; Conrey, 1967), may reach values of  $1 \text{ m}/10^3 \text{ y}$  (Scott and Williams, 1978). Assuming erosion rates and relief are dependent (Ahnert, 1970), a sediment source area perhaps 12 times the size of the basin (15 times, neglecting density differences between rock and sediment) is needed to fill the basin, based on the modern elevation of the San Gabriel Mountains. This scenario requires uplift of the source areas at a rate of  $1 \text{ km}/10^6 \text{ y}$  since the pulse of sedimentation occurred.

---

### Magnitude of Lithospheric Attenuation

---

Subsidence of the central block resulted from thinning of the lithosphere, and perhaps, some component of thermal subsidence, assuming that the basin is a pullapart basin. The magnitude of Late Miocene thinning may be estimated by comparing tectonic subsidence in the basin with the amount of subsidence predicted by isostasy. Uniform thinning of the lithosphere with depth, as in the McKenzie simple-stretching model (McKenzie, 1978), causes two types of subsidence. First, the lithosphere subsides due to the replacement of less dense crustal

material with more dense mantle material. This type of subsidence is referred to as the initial isostatic subsidence (McKenzie, 1978; Royden *et al.*, 1980) and occurs rapidly (depending primarily on the duration of rifting). Thermal subsidence caused by cooling of the lithosphere follows the initial subsidence and requires sufficient time for the lithosphere to approach thermal equilibrium.

Both the initial subsidence and thermal subsidence are dependent on the initial lithospheric thickness, density structure, and the magnitude of attenuation. Given that the lithosphere under the Los Angeles basin was 120 km thick, with a 35-km-thick crust (density 2.8 g/cc) and the remainder mantle (density 3.3 g/cc) before rifting, then stretching by a factor of 2 would result in an initial subsidence of 2.4 km. A stretching factor of 4 yields 3.6 km of initial subsidence. The computation of initial subsidence is given in BASIC in Appendix 2. Stretching by a factor of  $\beta$  is equivalent to thinning by a factor of  $1 - (1/\beta)$ . The maximum Pliocene to Recent tectonic subsidence in the central block is about 3 km. Thus, based on isostatic considerations alone, tectonic subsidence appears to be the result of stretching by a factor of 2-4 or thinning by 50-75% under the central deep.

A direct result of rifting, in the instantaneous-stretching model of McKenzie, is an increase in the geothermal gradient by a factor of  $\beta$ . The changes of temperature with time after rifting can be obtained by solving the one-dimensional heat-flow equation (Carslaw and Jaeger, 1959). Comparisons between predicted changes in heat flux with time for a given  $\beta$ , and actual heat flow (both modern and time-integrated, such as mirrored by vitrinite reflectance), may help in estimating  $\beta$ . The modern geothermal gradient in the central block is lower than in the adjacent blocks (Fig. 13-15). The lower geothermal gradient in the central block, which is about 27° C/km, may reflect the effect of high sedimentation rates, which depressed the geothermal gradient. Higher geothermal gradients in the other blocks of the Los Angeles basin may reflect the effect of rapid uplift; this would have brought hotter rocks closer to the surface, a more rapid way of transferring heat upward than by conduction.

## DISCUSSION

Many studies relevant to the history of the Los Angeles basin have been made, and many models have been proposed to explain the complex shifting of crustal blocks and crustal rotations in southern California (e.g., Jahns, 1973; Beck, 1976; Crouch, 1979b; Kammerling and Luyendyk, 1979; Sylvester and Darrow, 1979; Luyendyk *et al.*, 1980, Luyendyk and Hornafius, this volume). The main problems center on the long-term movement history of the San Andreas (Dickinson *et al.*, 1972; Nilsen and Clarke, 1975), post-Miocene crustal rotations (Luyendyk *et al.*, 1980; Luyendyk and Hornafius, this volume), and the timing of basin formation with respect to an evolving San Andreas. Rotations are very important because they impose a serious constraint on any kinematic model of basin formation. My purely speculative feeling is that rotations occur when upper-crustal slivers form by detachment from the lower crust, and rotate like ball-bearings between or perhaps above strike-slip faults. The magnitude of these rigid-body rotations is

# TEMPERATURE °C

50 100 150 200

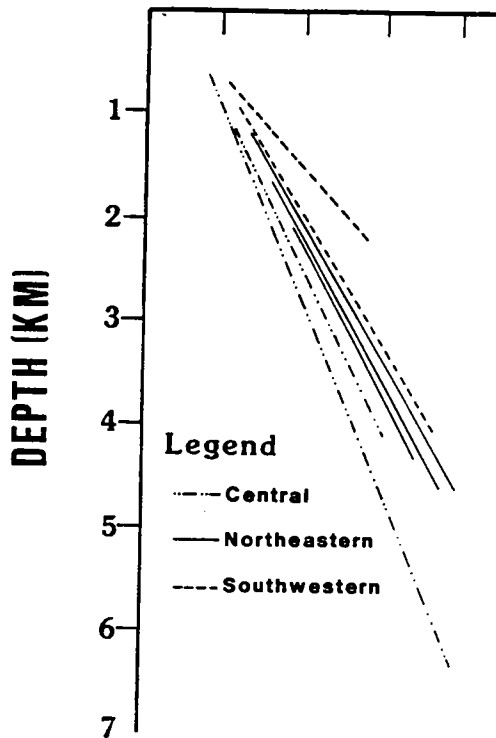


Fig. 13-15. Geothermal gradients in the Los Angeles basin Bostick, et al. (1978, 1979).

dependent not only on the slip of the faults, but also on the strength of the rocks that ultimately become penetratively sheared and fractured.

Importantly, there appears to be a tectonic sequence that consists of subsidence followed by uplift, typical of basins associated with the San Andreas in southern California. The Los Angeles, Ventura, Vallecito-Fish Creek, and Salton Trough basins are good examples of rapid subsidence followed by rapid uplift. This tectonic sequence may mean that pullapart regimes along the San Andreas are, by their very nature, transient and short-lived (e.g., Crowell, 1974a). Decoupling of upper and lower crust (or perhaps deeper) along the San Andreas, due to differences in the ability of these materials to accumulate stress, may be an important part of this process. The complex surface fault pattern of the San Andreas system, with concomitant basin formation, may represent the preserved record of deeper dynamic lithospheric structures of the San Andreas that have shifted or changed with time.

## ACKNOWLEDGMENTS

William R. Dickinson served as catalyst and reviewer for an earlier version of this

MAYER

317

317

manuscript and made many helpful suggestions. I thank Robert Yerkes for discussions on the Los Angeles basin. Also, I thank the editors of this volume for their most careful and patient editorial review. Jeanne Cooper assisted with drafting.

## APPENDIX 1: SLIP ON MAJOR FAULTS

### Regional Faults

Fault: San Andreas

Displacement: 305 km of right slip

Evidence: displaced geologic terranes

References: Crowell, 1962, 1968, 1971; Ross *et al.*, 1973; Nilsen and Clarke, 1975.

Notes: Present trace may be active from Pliocene only, with 108 km of right slip on proto-San Andreas (Graham, 1978). Change in pole of rotation about 10 my B.P. may have caused divergent wrenching (Silver, 1974).

Fault: San Gregorio-Hosgri

Displacement: 115 km of right slip

Evidence: correlation of offset features

References: Graham and Dickinson, 1976, 1978a,b; Graham, 1978.

Notes: Active post-Early Miocene, probably within the interval 15-5 my B.P.

Fault: Sur-Nacimiento

Displacement: uncertain amount of right slip

Evidence: offset Cretaceous plutons

Reference: Howell, 1975a

Fault: Rinconada-Reliz

Displacement: 43 km of right slip

Evidence: correlation of offset features

References: Dibblee, 1976; Blake *et al.*, 1978; Graham, 1978.

Notes: All movement is post-Oligocene and possible post-Early Miocene (Graham, 1979).

Fault: Big Pine

Displacement: 16 km of left slip

Evidence: Eocene facies changes, Sespe Formation not known north of the fault.

References: Hill and Dibblee, 1953; Woodford and Gander, 1977.

Fault: Garlock

Displacement: 48-64 km of left slip

Evidence: offset Permian Garlock Formation in El Paso Mountains and Pilot Knob Valley.

References: Smith and Ketner, 1970; Davis and Burchfiel, 1973.

Notes: Possibly active since about 30 my B.P.

## Faults Related to Los Angeles Basin

Fault: Newport-Inglewood

Displacement: 180-760 m of right slip

Evidence: laterally offset fold axes and oil-producing structures

References: Hill, 1971a; Harding, 1973.

Notes: The Lower Pliocene is involved in faulting (Yerkes *et al.*, 1965). Provenance indicates (based on Catalina Schist detritus) that faulting may have started during the Miocene.

Fault: Whittier-Elsinore

Displacement: 4.5 km of oblique slip or 5 km of right slip (since Miocene) 1.7 km of right slip (since Pleistocene)

Evidence: Down-to-southwest displacement in Puente Hills and offset stream courses. For southeast section of the Elsinore, offset cataclastic zone.

References: Yerkes *et al.*, 1965; Sharp, *in* Lamar, 1972.

Notes: May have significant pre-Miocene left slip (Woodford and Gander, 1977).

Fault: Santa Monica into Malibu Coast

Displacement: 80 km of left slip

References: Lamar, 1961; Yerkes *et al.*, 1965; Lang and Dreesen, 1975.

Notes: May have been inactive since latest Miocene (Lang and Dreesen, 1975).

Strike-slip movement accompanied by up to 2 km of north-side-up vertical displacement along Santa Monica section and 1.1 km along Raymond Hill section of the fault (Yerkes *et al.*, 1965).

Fault: Malibu-Cucamonga

Displacement: 90 km of left-slip (during Middle Miocene ?)

Evidence: displaced source terranes of Chico Formation

References: Yerkes and Campbell, 1971; Carey and Colburn, 1978.

Notes: Restoration of displacement places Santa Monica block directly north of the Peninsular Ranges. This is consistent with paleocurrents from the Trabuco which indicate a southern source. There is no Franciscan-like detritus in the upper Chico (Carey and Colburn, 1978). Clockwise rotation of the Santa Monica Slate is compatible with its detrital compositions (Jones and Irwin, 1975)

## APPENDIX 2: CALCULATION OF INITIAL SUBSIDENCE

5 'WRITTEN IN MICROSOFT BASIC

10 CLS: 'WORKS ON MOST VERSIONS, DELETE #10 IF PROBLEM

20 CALL TEXTFONT(0):' # 20 FOR MACINTOSH ONLY

30 PRINT" \_\_\_\_\_"

40 PRINT:PRINT" INITIAL SUBSIDENCE CAUSED BY RIFTING"

50 PRINT " BASED ON MCKENZIE (1978) , EPSL"

60 PRINT" \_\_\_\_\_"

70 PRINT:PRINT:PRINT

MAYER

319

308

```

80 INPUT "Lithosphere thickness";A
90 INPUT "Crustal thickness";TC
100 INPUT "Stretching factor";B
110 PRINT:PRINT
120 G=(1-(1/B))
130 U=-1*A*G*(.5*(TC/A)*(1-(.039*TC/2*A))-.039*3.3/2)
140 U=U/(3.3*(1-.00003*1300)-1.03)
150 PRINT"          LITHOSPHERE=";INT(A);" KM THICK"
170 PRINT"          CRUST=";INT(TC);" KM THICK":PRINT
180 GG=INT(100*G) /100
190 PRINT"          BETA=";B;" OR GAMMA=";GG
200 U=INT(1000*U) /1000
210 PRINT"          SUBSIDENCE=";U
220 THIS PROGRAM USES:
230 '   MANTLE DENSITY OF 3.3 G/CC   WATER DENSITY OF 1.03 G/CC
240 '   CRUSTAL DENSITY OF 2.8 G/CC   TEMP AT BASE OF LITHOSPHERE=1300C
250 '   COEFFICIENT OF THERMAL EXPANSION= 3E-5

```

320